Biochemical analysis of cell-derived apoE3 particles active in stimulating neurite outgrowth

Ronald B. DeMattos,[1,*] Lawrence L. Rudel,[†] and David L. Williams[2,*]

Department of Pharmacological Sciences,* University Medical Center, State University of New York at Stony Brook, Stony Brook, NY 11794; and Department of Pathology (Comparative Medicine),† Wake Forest University School of Medicine, Winston-Salem, NC 27103

Abstract Susceptibility to the development of late-onset Alzheimer's disease is increased for individuals harboring one or more apolipoprotein E4 (apoE4) alleles. Although several isoform-specific effects of apoE have been identified, the relationship between biochemical function and risk factor assessment is unknown. Our previous studies showed that a physiologically relevant cell-derived apoE3 particle stimulates neurite outgrowth in an isoform-specific manner. In an attempt to delineate the biochemical mechanism responsible for the stimulatory effects of apoE3 on neurite outgrowth, we performed a detailed physical characterization of cell-derived apoE3 and apoE4 particles. Immunoaffinity chromatography followed by SDS-PAGE illustrated homogeneity in protein content (apoE >95%). The affinity-purified particles contained phospholipid and 1 mol of cholesterol per mole of apoE but no core lipids. Nondenaturing gradient gel electrophoresis identified two major particle populations with hydrated diameters of 8.0 and 9.2 nm. Neurite outgrowth assays performed with the affinity-purified particles resulted in similar isoform-specific differences as seen previously, apoE3 stimulatory and apoE4 neutral. Interestingly, we did not observe a reduction in apoE medium concentrations over the duration of the neurite outgrowth assays, suggesting little or no endocytic uptake. Ligand blot analysis demonstrated that the affinity-purified apoE particles bind to several Neuro-2a membrane proteins. Western blots of the Neuro-2a membrane proteins indicated that the LDL receptor, gp330, and LR8B might be involved in the apoE-binding event. These results discriminate against the lipid delivery hypothesis and suggest that the biological activity of the phospholipid apoE3 particles may be due to cell surface signaling.—DeMattos, R. B., L. L. Rudel, and D. L. Williams. **Biochemical analysis of cell-derived apoE3 particles active in stimulating neurite outgrowth.** ***J. Lipid Res.*** **2001.** 42: **976–987.**

Supplementary key words Alzheimer's disease • HDL • LDL receptor • LDL receptor-related protein • neurodegeneration • cholesterol

Apolipoprotein E (apoE) was first discovered in 1973 by Shore and Shore (1) as an arginine-rich protein constituent of triglyceride-rich VLDL. Early studies identified apoE as a key component of plasma cholesterol homeostatic mechanisms (2). It was demonstrated that apoE, a 299-amino acid secretory protein, bound with high affinity to lipoprotein particles in the plasma compartment and acted as a ligand for receptor-mediated endocytosis via multiple members of the LDL receptor family (3). The expression of apoE is quite diverse as compared with most other members of the apolipoprotein family, which are mainly of hepatic or intestinal origin. ApoE is expressed at particularly high levels in liver, brain, and steroidogenic tissues (4–7). The secretion and association of apoE with nascent hepatic lipoproteins have been investigated thoroughly (8), yet only a few reports have focused on the lipoprotein nature of apoE secreted by nonhepatic cells (9–12). There are three common isoforms of apoE that result from cysteine-arginine interchanges at residues 112 and 158 (13). The most common isoform, apoE3, has a cysteine at residue 112 and an arginine at residue 158. ApoE4 contains two arginines, whereas apoE2 contains cysteines at these positions.

Unlike the role of apoE in the plasma compartment, the function of apoE in the central nervous system remains obscure. Brain apoE is secreted by astrocytes and microglial cells (14–17) and attains a steady state concentration in the cerebral spinal fluid of 5% to 10% of that in the plasma (5–10 μg/ml) (18, 19). A dramatic increase in apoE expression in response to nerve damage led to the hypothesis that apoE was involved in the processes of neuronal repair and remodeling through the reuse of cholesterol and lipid, a function analogous to that of plasma apoE (6, 20–23). The importance of delineating the role of brain apoE was heightened after it was discovered to be involved in the onset and progression of Alzheimer's disease (24–27). Genetic studies have identified the ε4 allele of apoE as a risk factor for the development of late-onset and sporadic Alzheimer's disease (24–27). The biochemical basis for this correlation remains unknown. Several avenues of research have attempted to identify a biological role of brain apoE that is

Abbreviations: apo, apolipoprotein; NDGGE, nondenaturing gradient gel electrophoresis.

[1] Present address: Department of Neurology, Center for the Study of Nervous System Injury, Washington University School of Medicine, 660 South Euclid Avenue, Box 8111, St. Louis, MO 63110.

[2] To whom correspondence should be addressed.
e-mail: dave@pharm.sunysb.edu

sensitive to isoform-specific modulation. These lines of research focus on the role of apoE in amyloid fibrillogenesis/deposition (28–32), cytoskeletal modulation/tau phosphorylation (27, 33, 34), and neuronal plasticity (35–38).

ApoE3 has been shown to stimulate neurite outgrowth in an isoform-specific manner in several culture systems (35–38). Handelmann et al. (39) were the first to demonstrate an effect of apoE on neurite outgrowth. Cultures of dorsal root ganglion neurons exhibited a decrease in neurite branching and a stimulation of neurite outgrowth when incubated with delipidated rabbit apoE plus β-VLDL. It was hypothesized that the stimulation in neurite outgrowth was due to enhanced lipid delivery. A similar study using a murine neuroblastoma cell line, Neuro-2a, showed that human apoE altered neurite morphology in an isoform-specific manner (35). Addition of delipidated apoE3 plus β-VLDL stimulated neurite outgrowth, whereas apoE4 plus β-VLDL was inhibitory. Studies by Fagan et al. (40) showed a similar isoform-specific effect with GT1-1 trk9 cells, an immortalized hypothalamic neuronal cell that was stably transfected with the nerve growth factor receptor trkA. Cells incubated in the presence of apoE3-enriched human HDL and nerve growth factor had a dramatic increase in neurite outgrowth. The stimulatory effects of the apoE3-HDL were inhibited by the addition of antibodies to the LDL receptor-related protein (LRP). In addition, it was shown in several studies that the apoE3 stimulation of neurite outgrowth was receptor-associated protein (RAP) sensitive, thereby implicating a critical role of the members of the LDL receptor (LDLR) superfamily of receptors (36, 38, 40, 41). Interestingly, the stimulatory effects of apoE in each of these studies could be demonstrated only after lipoproteins were further enriched with exogenous human apoE, despite the fact that each lipoprotein already contained abundant apoE protein (rabbit apoE for the β-VLDL studies and human apoE for the cerebrospinal fluid studies). Although these studies did not identify the stimulatory mechanism of apoE in neurite outgrowth, the results were consistent with the lipid delivery hypothesis.

Our previous studies showed that a minimally lipidated form of cell-derived apoE exhibited isoform-specific stimulation of neurite outgrowth (37). Importantly, the isoform-specific effect did not depend on the addition of exogenous lipids or lipoproteins. Neuro-2a cells secreting apoE3 developed neurite extensions that were significantly longer than the parent Neuro-2a cells or Neuro-2a cells expressing apoE4. Preliminary analysis of the cell-derived apoE isoform by density gradient ultracentrifugation showed it to be in a poorly lipidated particle with a density between 1.19 and 1.26 g/ml. These results demonstrated that the biological activity of apoE3 did not depend on either an interaction of apoE3 with exogenous lipid sources or independent actions of apoE3 and β-VLDL. In the present report, we further characterize the cell-derived apoE3 and apoE4 particles in an attempt to identify the mechanism responsible for the isoform-specific stimulation in neurite outgrowth. We demonstrate that apoE is the only detectable protein in affinity-purified particles and that the particles are small HDL-like lipoproteins composed predominantly of apoE and phospholipid. There is little or no endocytosis of the apoE particles. This result as well as the absence of core lipids argues strongly against the lipid delivery hypothesis. These findings raise the possibility that the apoE3-mediated stimulation of neurite outgrowth is due to signals generated at the cell surface. Ligand and Western blot analyses identified several LDLR family members that could potentially initiate these signals.

EXPERIMENTAL PROCEDURES

Cell culture

Neuro-2a cells were maintained in a 37°C humidified 95% air/5% CO_2 incubator in medium A [DMEM-F12 (1:1) supplemented with 10% heat-inactivated fetal bovine serum (FBS) (Atlanta Biologicals, Norcross, GA), 4 mM glutamine, penicillin (100 U/ml), streptomycin sulfate (100 U/ml), and amphotericin B (0.25 μg/ml)]. The clonal lines 1B (apoE3) and 1E4A (apoE4) were used for all apoE experiments (37). The transfected cell lines were grown in the presence of G418 (350 μg/ml). Cell lines were maintained between 20% and 70% confluent between experiments.

Affinity purification of apoE lipoproteins

Conditioned medium was prepared as follows: Neuro-2a 1B (apoE3) and Neuro-2a 1E4A (apoE4) cells were split 1:6 from a 95% confluent 175-cm^2 flask into six 175-cm^2 flasks and incubated in medium A for 24 h. After a change of medium and a continued 12-h incubation, the cells were washed once with basal medium (medium A lacking FBS) and were incubated for 24 h in 70 ml of basal medium (conditioning medium). The conditioned medium was spun at 2,500 *g* for 30 min at 4°C to remove cellular debris. The medium was transferred to a sterile 500-ml bottle, sodium azide was added to a final concentration of 0.02%, and the medium was immediately used for particle isolation at 4°C.

Conditioned medium (420 ml) for either apoE3 or apoE4 was passed twice over a monoclonal antibody column at a flow rate of ~1 ml/min at 4°C. The affinity columns consisted of 40 mg of the monoclonal antibody 1E (37) coupled to 4 ml of Sepharose 4B. Separate columns were used for apoE3 and apoE4 particle isolations. The columns were washed with 100 ml of PBS plus 0.02% sodium azide, and the apoE-containing particles were eluted in 3 M sodium thiocyanate. Fractions containing the eluted apoE particles were dialyzed against six changes of 4 liters of sterile PBS six times over a 24-h period at 4°C. A mock elution of 3 M sodium thiocyanate was dialyzed in tandem with the eluted apoE particles. The resulting preparations are referred to as affinity-purified apoE particles. For some experiments, the affinity-purified apoE particles were subjected to heparin affinity chromatography as follows: Eluted apoE was diluted with 500 ml of 25 mM Tris (pH 8.0)-50 mM ammonium bicarbonate and recycled over a 5-ml heparin-agarose column (Pharmacia, Piscataway, NJ) at 2 ml/min for 12 h. After the column was washed with 50 ml of PBS, the heparin-bound apoE was eluted with 1 M ammonium bicarbonate. ApoE-containing fractions were then dialyzed extensively against PBS at 4°C as stated above. A mock elution for either type of chromatography (antibody or heparin) was dialyzed in parallel and used as the control in neurite outgrowth studies. The affinity-purified apoE particles and heparin-binding particles were dialyzed overnight into basal medium and

were sterilized by filtration through preblocked [1% bovine serum albumin (Sigma, St. Louis, MO) in PBS] 0.2 μm pore size filters (Schleicher & Schuell, Keene, NH).

Characterization of the affinity-purified apoE particles

The concentration of the affinity-purified and heparin-purified apoE particles was determined by ELISA, using a commercially available apoE standard (PanVera, Madison, WI) as previously described (37). The protein heterogeneity of the isolated apoE particles was evaluated by SDS-PAGE. Ten micrograms of the isolated apoE particles (heat denatured and reduced) was run on a 10% SDS-polyacrylamide gel and subsequently stained with Coomassie blue. ApoE Western blots were performed as previously described (37).

Nondenaturing gradient gel electrophoresis (NDGGE) was used to evaluate the particle size heterogeneity of the apoE fractions. Large (16 cm × 14 cm × 1.5 mm) TBE (pH 8.3)-buffered polyacrylamide gradient gels (4% to 25%) were prerun at 125 V for 30 min at 4°C. The lower chamber of the electrophoresis unit was completely filled with TBE, pH 8.3, to maintain the gel at 4°C. Pharmacia native high molecular weight protein standards (50 μg per lane) were used as size standards (42). ApoE particles (nonboiled and nonreduced) were loaded in a buffer containing 10% sucrose-0.016% bromphenol blue. Electrophoresis was performed with the following step voltage scheme: 25 V for 15 min, 50 V for 15 min, 75 V for 15 min, and 250 V for 24 h. The proteins were electrophoretically transferred from the polyacrylamide gel to a nitrocellulose membrane at 200 mA for 12 to 16 h at 4°C. The membrane was then stained with 0.1% Ponceau S-5% acetic acid, and the locations of the proteins in the standard lane were marked with pencil. Immunodetection of the apoE on the membrane was performed with a polyclonal goat anti-human apoE antibody (BioDesign International, Saco, ME) as previously described (37).

Lipid analysis of the affinity-purified apoE particles was performed essentially as described (43). Briefly, samples were subjected to a Bligh-Dyer extraction and 0.5ml aliquots were removed and dried under N_2. The sample was dissolved in 100 μl of $CHCl_3$ and was spotted onto a 10 × 10 cm high performance thin-layer chromatography plate (HPTLC; EM Science, Gibbstown, NJ), using a 0.1 ml CAMAG (Wilmington, NC) Linomat syringe. Fatty acid analysis was conducted as previously described (44, 45).

Neurite extension assay

Neuro-2a cells were trypsinized and plated at low cell densities on days −4 and −2. At time 0 cells were trypsinized for exactly 2 min and subsequently plated at a density of 4.0×10^3 cells per well of a 12-well tissue culture plate (Costar, Cambridge, MA) in medium A. After 2 h at 37°C, medium was removed, the dish was washed once with basal medium (medium A lacking FBS), and a 30 μg/ml concentration of apoE3, apoE4, or mock elution, each containing 1× N2 supplement (GIBCO-BRL, Gaithersburg, MD), was added. After 48 h of incubation at 37°C, cells were fixed in PBS containing 2.5% glutaraldehyde for 30 min at room temperature. Each well was washed three times with PBS and images were collected with a ×16 phase-contrast objective. Images were analyzed with the UTHSCSA Image Tool program (developed at the University of Texas Health Science Center at San Antonio, TX and available from the internet by anonymous FTP from http://www.UThscsa.edu/dig/download.html). Every cell that contained a process longer than the cell diameter was measured (longest neurite only). All microscopy experiments were coded before image acquisition and again before neurite measurements (double-blind coding procedures).

ApoE ligand blot analysis and Neuro-2a receptor survey

Affinity-purified apoE particles were used to screen Neuro-2a membrane proteins to identify potential apoE receptors. Neuro-2a cells were grown in 10-cm dishes in medium A until 80% confluent. The dishes were then changed into basal medium plus N2 supplements for 16 h. After three washes with PBS, cells were scraped in PBS from the dishes and were homogenized with a Dounce homogenizer on ice. Cell lysates were spun at 12,000 *g* for 20 min at 4°C. The resulting supernatant was spun at 100,000 *g* for 1.5 h at 4°C. Membrane proteins in the pellet were resuspended in 1% Triton X-100 and the protein concentration was determined by the method of Lowry et al. (46), using IgG as standard. Large 4% to 8% SDS-polyacrylamide gradient gels were poured, using a two-chamber gradient maker. Pharmacia high molecular weight protein standards (50 μg per lane) were used as size standards. Nonboiled membrane proteins (200 μg for ligand blots or 100 μg for Western blots) in nonreducing SDS sample buffer were run at 150 V for ~7 h. The proteins were electrophoretically transferred from the polyacrylamide gel to a nitrocellulose membrane at 300 mA for 16 h at 4°C. Ponceau S staining identified the locations of the proteins in the standard lane. The membrane was cut into strips and used for apoE ligand blotting or for a Western blot receptor survey.

Ligand blots. Each strip was blocked for 1 h at room temperature in 50 mM Tris-HCl (pH 7.4), 100 mM NaCl, and 2 mM $CaCl_2$ (BB) containing 10% nonfat milk. The strips were rinsed once in BB and were incubated with apoE particles (1 μg/ml) in BB containing 1% nonfat milk (BBM) for 1 h at room temperature with gentle rocking. The nitrocellulose strips were then washed for 1 h with four changes of BBM. ApoE was detected by incubating the strips in BBM containing an affinity-purified polyclonal goat anti-human apoE antibody (BioDesign International) at 2 μg/ml for 1 h at room temperature. Strips were washed three times with BBM and incubated with a horseradish peroxidase-conjugated anti-goat IgG (Sigma) for 1 h at room temperature in BBM. The bands were visualized by enhanced chemiluminescence (Pierce, Rockford, IL).

Receptor sur vey. The nitrocellulose membranes were blocked for 1 h at room temperature in 20 mM Tris-HCl (pH 7.4), 150 mM NaCl, and 0.02% Tween 20 (TBST) containing 7% nonfat milk. The blocked membranes were then incubated with one of the following primary antibodies in TBST containing 1% nonfat milk: anti-LRP (4 μg/ml; R777), anti-VLDL receptor (VLDLR) (4 μg/ml; R2623), anti-gp330 (4 μg/ml; R784), anti-LDLR (1:500; R4526), and anti-LR8B (1:500; α-20). Antibodies R777, R2623, and R784 were generous gifts from D. K. Strickland (American Red Cross, Holland Laboratory, Rockville, MD) and the α-20 antibody was a generous gift from J. Nimpf (University of Vienna, Vienna, Austria). The membrane was washed three times with TBS containing 0.05% Tween 20 and incubated with a horseradish peroxidase-conjugated anti-goat IgG (Sigma) for 1 h at room temperature in TBS containing 1% nonfat milk and 0.05% Tween. Bands were visualized by enhanced chemiluminescence (Pierce).

RESULTS

Particle characterization

Our previous studies demonstrated that the murine neuroblastoma cell line Neuro-2a exhibits an apoE isoform-specific stimulation in neurite outgrowth (37). Neuro-2a cells stably transfected with apoE3 had significantly longer neurites compared with apoE4 transfected or parental

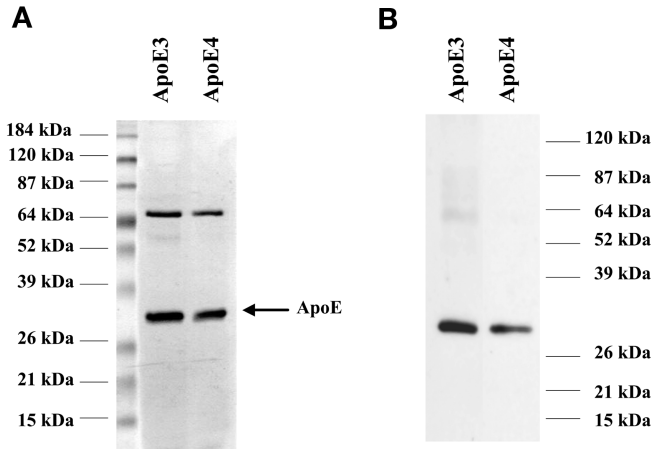

Fig. 1. SDS-PAGE analysis of affinity-purified apoE particles. Affinity-purified apoE3 and apoE4 were isolated from conditioned medium of transfected Neuro-2a cells as described in Experimental Procedures. A: Affinity-purified apoE3 and apoE4 (10 μg) were heat denatured and reduced before separation on a 10% SDS-polyacrylamide gel. Proteins were visualized by Coomassie blue staining. B: Purified apoE3 and apoE4 (100 ng) were electroblotted to a nitrocellulose membrane after 10% SDS-PAGE and the membrane was probed with an affinity-purified polyclonal goat anti-human apoE antibody. After incubation with a horseradish peroxidase-conjugated anti-goat IgG, bands were visualized by enhanced chemiluminescence. Prestained Benchmark protein ladders (GIBCO-BRL) were used for molecular weight assessment.

cells. ApoE3 affinity purification and subsequent neurite outgrowth studies showed that the biological activity was inherent to the secreted apolipoprotein. To elucidate the biological mechanism underlying the isoform-specific stimulation of neurite outgrowth, we characterized the secreted apoE particles. ApoE3 and apoE4 were affinity purified from conditioned medium on monoclonal antibody columns. The isolated apolipoproteins were first analyzed by SDS-PAGE to identify the protein constituents. Coomassie blue staining reveals that greater than 95% of the eluted protein is present as a 36-kDa polypeptide (**Fig. 1A**). Note that the band located at 67 kDa is bovine serum albumin that is added exogenously during the purification procedure. Western blot analysis confirms that the 36-kDa polypeptide is apoE (Fig. 1B). In addition, the minor higher molecular weight bands seen in the Coomassie gel are apoE immunoreactive. Thus, the sole protein component of the eluted material is apoE.

The affinity-purified apoE particles were subjected to lipid analysis. Our previous study indicated that the secreted apoE was present as a minimally lipidated particle that floated between densities 1.19 to 1.26 g/ml. **Table 1** shows that the main lipid of the purified particles is phospholipid with trace amounts of free cholesterol. Interestingly, the measurements indicate one molecule of cholesterol per molecule of apoE. Core lipids (cholesteryl ester or triglyceride) were not detected. The lack of core constituents and the presence of a high phospholipid content are suggestive of discoidal apoE lipoproteins (47). Fatty acid analysis (**Table 2**) of the apoE particles showed a typical acyl chain distribution that is consistent with common phospholipid classes (even distribution of saturated and unsaturated acyl chains) (48). No significant differences ($P > 0.05$) in lipid composition (Table 1) or acyl chain composition (Table 2) were seen between the apoE3 and apoE4 isolated particles.

The sizes of the lipoprotein particle populations were analyzed by NDGGE (41). Conditioned medium and affinity-purified apoE3 and apoE4 particles were separated by NDGGE and subsequently analyzed by apoE Western blotting (**Fig. 2A**). Two prominent apoE particle populations with diameters of 8.0 and 9.2 nm and several minor particle populations (7.6, 10.4, 12.2, and 17.0 nm) were present in conditioned medium for both apoE3 and apoE4. The same particle populations were seen in affinity-purified apoE preparations, indicating that the isolation procedure did not alter the apoE particle distribution. This technique is not adequate to assess the relative apoE particle concentrations because of variable transfer efficiencies for the lipoproteins of different size. Because our preparations are composed solely of apoE, a more appropriate measure is to analyze the particles before transfer. Fifteen micrograms of isolated apoE3 particles was subjected to NDGGE and stained with Coomassie blue (Fig. 2B). The apoE protein is mainly localized to two particle populations with hydrated diameters of 8.0 and 9.2 nm (the 7.1-nm band represents the exogenously added serum albumin). We further confirmed that the protein components of the 8.0- and 9.2-nm bands contain only apoE by a two-dimensional gel analysis (Fig. 2C). Affinity-purified particles were separated by

TABLE 1. Lipid composition of affinity-purified apoE particles

Particle	ApoE	Phospholipid	Cholesterol	Cholesterol Ester	Triglyceride
	μg (M)	*μg (M)*	*ng (M)*		
ApoE3	1 (1)	6.3 ± 0.7 (298)	11.4 ± 3.4 (1.0)	ND (0)	ND (0)
ApoE (heparin)	1 (1)	4.5 ± 2.2 (213)	11.9 ± 4.8 (1.1)	ND (0)	ND (0)
ApoE4	1(1)	8.8 ± 1.2 (417)	13.7 ± 4.6 (1.2)	ND (0)	ND (0)
ApoE4 (heparin)	1(1)	6.2 ± 0.7 (294)	12.5 ± 2.5 (1.1)	ND (0)	ND (0)

ApoE3 and apoE4 particles were purified by immunoaffinity chromatography from conditioned medium and further fractionated by heparin-agarose chromatography (where indicated) as described in Experimental Procedures. ApoE content was determined by ELISA and the lipid content was determined by HPTLC, results are reported as mass ± standard error relative to apoE set at 1. Values in parentheses are calculated molar values relative to apoE. Five individual isolations for the affinity-purified particles and three isolations for the heparin-purified particles were evaluated. No significant differences ($P > 0.05$) were observed between the apoE3 and apoE4 particle preparations. ND, not detected.

TABLE 2. Phospholipid acyl chain composition of apoE particles

Fatty Acid	Fatty Acid Composition	
	ApoE3	ApoE4
12:0	1.9 ± 0.7	1.9 ± 0.6
14:0	5.1 ± 0.2	3.6 ± 1.3
15:0	1.5 ± 0.0	1.3 ± 0.2
16:0	31.1 ± 0.4	28.0 ± 0.4
18:0	13.2 ± 2.3	14.5 ± 0.4
20:0	0	0
16:1	4.9 ± 0.6	3.7 ± 0.2
18:1	27.2 ± 3.3	31.0 ± 0.9
18:2	4.2 ± 1.0	4.1 ± 1.0
20:4	4.6 ± 0.5	5.0 ± 1.2
22:1	0.6 ± 0.8	0.5 ± 0.8
22:4	3.2 ± 1.8	3.9 ± 0.6
22:5	1.0 ± 0.4	0.8 ± 1.1
22:6	1.5 ± 0.4	1.7 ± 0.5

Two independent preparations of affinity-purified apoE particles were analyzed to determine the fatty acyl chain composition as described in Experimental Procedures. The values shown are the mean percent distribution (±SD) for each apoE isoform. No significant differences ($P > 0.05$) were observed between the apoE3 and apoE4 particle preparations.

NDGGE (first dimension) followed by SDS-PAGE in the second dimension. This analysis showed that the 8.0- and 9.2-nm bands contain only the 36-kDa apoE. These results demonstrate that the majority of the apoE is present as HDL-sized phospholipid particles.

Biological activity

The biological activity of the affinity-purified apoE3 and apoE4 phospholipid particles was evaluated in neurite outgrowth assays. Parental Neuro-2a cells were incubated with a 30 μg/ml concentration of either apoE3 or apoE4 particles for 48 h and subsequently analyzed for neurite outgrowth. **Figure 3A** shows that Neuro-2a cells incubated in the presence of apoE3 maintain longer neurites over the entire population, whereas cells incubated with apoE4 were similar to the control. When analyzed for average neurite lengths (Fig. 3B), the apoE3-treated cells had significantly longer neurites (164%, $P = 0.0001$ vs. control). No significant change in neurite outgrowth was detected for cells treated with the affinity-purified apoE4, confirming our previous observation in stably transfected Neuro-2a cells that apoE4 is neutral for neurite outgrowth (37). ELISA measurement of apoE mass in the medium at the conclusion of the 48-h assay showed no difference from initial concentration (data not shown). We also analyzed the apoE particle populations present at the conclusion of a 48- and 96-h assay by NDGGE apoE Western blot (**Fig. 4**). Neither particle concentration nor the distribution of the particle populations for apoE3 and apoE4 was altered after incubation with cells for either 48 or 96 h. Note that we have shown previously that Neuro-2a-derived apoE3 is effective in mediating rapid endocytosis when the apoE is purified and reconstituted into large dimyristoylphosphatidylcholine disks or added to β-VLDL particles from apoE-deficient mice (33). The lack of endocytosis observed here, therefore, likely reflects the presence of apoE in small particles that are not efficiently taken up by receptor-mediated endocytosis.

Because several previous studies have demonstrated the importance of heparan sulfate proteoglycans in the bind-

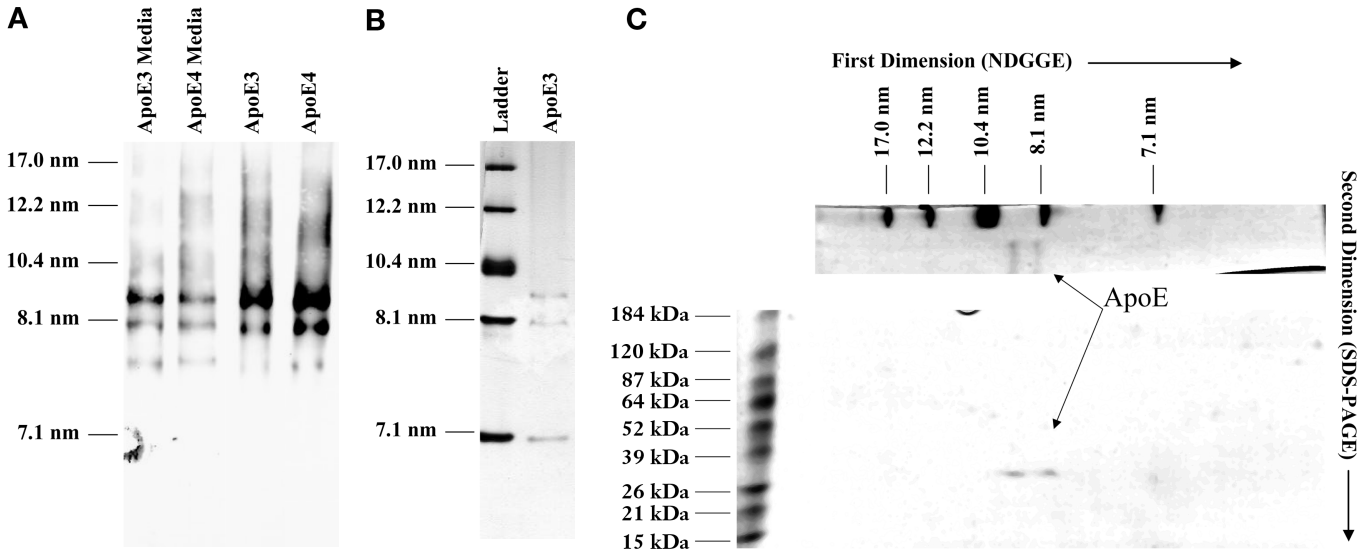

Fig. 2. Nondenaturing gradient gel analysis of affinity-purified apoE particles. The native size heterogeneity of the purified particles was determined by NDGGE. A: Conditioned media and purified particles for apoE3 and apoE4 (200 ng), nondenatured and nonreduced, were run through a 4–25% TBE gradient gel and were electroblotted to a nitrocellulose membrane. The membrane was then probed with an affinity-purified polyclonal goat anti-human apoE antibody. After incubation with a horseradish peroxidase-conjugated anti-goat IgG, bands were visualized by enhanced chemiluminescence. Pharmacia native high molecular weight standards were used for hydrated diameter assessment. B: Affinity-purified apoE3 particles (15 μg) were separated by NDGGE and the proteins were visualized by Coomassie blue staining. C: To verify that the protein composition of the 8.0- and 9.2-nm particles was 36-kDa apoE, affinity-purified apoE3 particles were analyzed in two dimensions as described in Experimental Procedures. First, apoE3 particles (17.5 μg) were separated by 4–25% NDGGE as described above (first dimension). The polyacrylamide lane containing the separated particles was then subjected to reducing 4–20% SDS-PAGE (second dimension). Proteins were visualized by Coomassie blue staining.

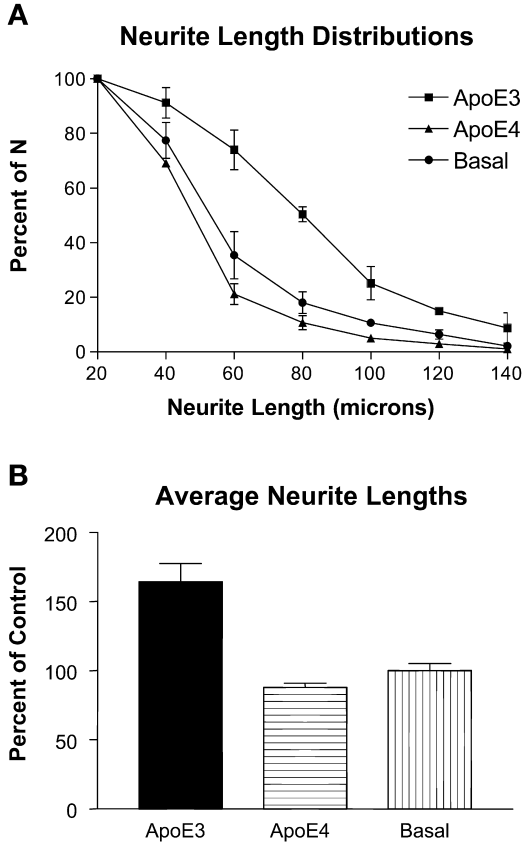

Fig. 3. Effect of affinity-purified apoE phospholipid particles on neurite outgrowth in Neuro-2a cells. Neuro-2a cells were incubated with N2-supplemented control medium (dialysis/bovine serum albumin control), or in the presence of a 30 μg/ml concentration of affinity-purified apoE3 or apoE4 for 48 h. Multiple phase-contrast images were captured with a ×16 objective and analyzed with the Image Tool program. Neurite extensions were determined by measuring the longest neurite from at least 50 responsive cells in duplicate experiments. A: The data were analyzed to determine the percentage of Neuro-2a cells (N) expressing neurites of defined lengths. Error bars indicate the standard deviation. B: Average neurite lengths were calculated and are shown as a percentage of control (set to 100%). The error bars indicate the standard error. The level of significance of the difference between apoE3-treated cells and control was $P = 0.0001$.

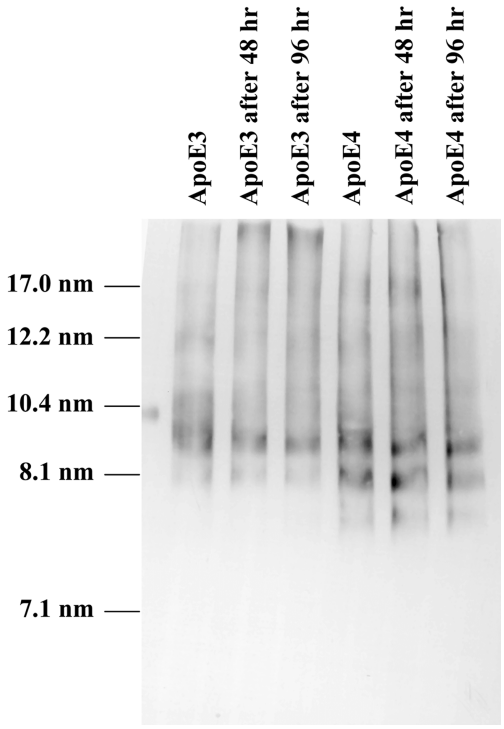

Fig. 4. Nondenaturing gradient gel analysis of affinity-purified apoE3 and apoE4 particles before and after incubation with Neuro-2a cells. Equivalent volumes of medium containing affinity-purified apoE3 and apoE4 particles (500 ng) before and after incubation (48 and 96 h) with Neuro-2a cells were run through a 4–25% TBE gradient gel. The proteins were transferred to a nitrocellulose membrane and probed with an affinity-purified polyclonal goat anti-human apoE antibody. After incubation with a horseradish peroxidase-conjugated anti-goat IgG, bands were visualized by enhanced chemiluminescence. Pharmacia native high molecular weight standards were used for hydrated diameter assessment.

ing of apoE-containing lipoproteins to some cell surface receptors as well as for direct binding of apoE particles to the cell surface (49–52), we analyzed the capacity of the apoE particles to bind heparin and tested whether they retained biological activity. Antibody-purified apoE3 and apoE4 were subjected to heparin chromatography and the eluted particles (heparin apoE3 or apoE4) were tested in neurite outgrowth assays. Both antibody-purified apoE3 and apoE4 readily bound to heparin-agarose columns. ApoE Western analysis of nondenaturing gradient gels showed no difference in particle populations between antibody-purified apoE and heparin apoE (**Fig. 5**). Neurite outgrowth assays performed with heparin apoE3 and apoE4 yielded results similar to those seen with the antibody-purified preparations (**Fig. 6**). The heparin apoE3 particles had longer neurite distributions (Fig. 6A) and significantly longer average neurite lengths (Fig. 6B) when compared with control cells (142%, $P = 0.008$). It must be noted that in some extension assays the biological activity of apoE3 was lost. In some cases we could attribute the loss of activity to microbial contamination, but our impression is that the biological activity may also be lost on extensive handling during purification. Nevertheless, it is clear that the biologically active apoE3-phospholipid complex has an affinity for heparin.

ApoE ligand blot and receptor survey

An intriguing question from these studies is, by what mechanism do the apoE3 phospholipid particles stimulate neurite outgrowth? A popular hypothesis has been the lipid delivery model (6, 20–23), yet our results showing a biologically active core-free apoE3 particle diminish the likelihood of this model. A more likely possibility is that apoE activates a cellular signaling pathway, a model requiring that the apoE-phospholipid complex would have to be competent to bind to cellular receptors. Previous studies using exogenously added RAP showed that the apoE3 stimulation of neurite outgrowth is dependent on members of the LDLR superfamily of receptors (36, 38, 40, 41). Although it has been shown that lipid-free apoE binds poorly to some receptors (47), little is known about

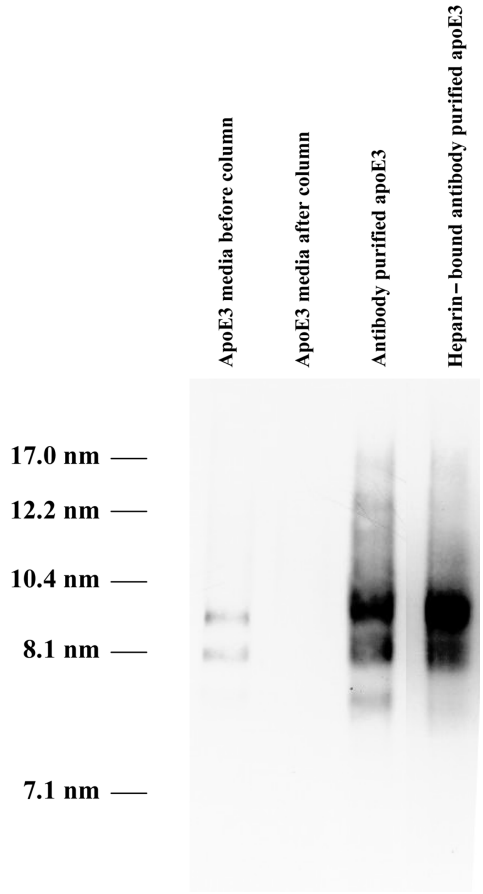

Fig. 5. Nondenaturing gradient gel analysis of heparin-binding apoE3 and apoE4 particles. Affinity-purified apoE3 particles were subjected to heparin affinity chromatography as described in Experimental Procedures. Conditioned media before and after antibody affinity purification, antibody affinity-purified apoE3, and heparin-bound antibody-purified apoE3 (200 ng) were run a through a 4–25% TBE gradient gel. The proteins were transferred to a nitrocellulose membrane and probed with an affinity-purified polyclonal goat anti-human apoE antibody. After incubation with a horseradish peroxidase-conjugated anti-goat IgG, bands were visualized by enhanced chemiluminescence. Pharmacia native high molecular weight standards were used for hydrated diameter assessment.

the receptor competency of the small apoE-phospholipid complexes described above. We performed ligand blots with the affinity-purified apoE particles to test for binding to Neuro-2a membrane proteins. Membrane proteins were isolated from Neuro-2a cells grown under conditions similar to those used in the neurite outgrowth assays (N2 differentiated). Nonheated/nonreduced membrane proteins were separated on large 4–8% SDS-polyacrylamide gels and transferred to nitrocellulose. **Figure 7A** demonstrates that the apoE3 and apoE4 particles bound to only a few membrane proteins. There is specificity in this interaction because several high abundance membrane proteins, identified by Ponceau S staining of the nitrocellulose membrane, did not bind the apoE particles. The prominent apoE-binding bands had apparent molecular masses of 280, 212, 206, 167, and 147 kDa. No reproducible differences were seen between apoE3 and apoE4 particles.

Next, we performed an LDLR family survey with antibodies to LRP, gp330, LDLR, LR8B/apoER2, and VLDLR on the isolated membrane proteins to identify any potential candidate apoE receptors (Fig. 7B). Immunoreactive bands for gp330, LDLR, and LR8B/apoER2 were apparent, whereas no signal was detected for LRP or VLDLR. The calculated molecular weight of the immunoreactive bands for the LDLR and LR8B/apoER2 (167 and 126 kDa, respectively) correlate well with reported literature values (53, 54). In addition to the major immunoreactive band at 126 kDa, there were two less prominent reactive bands at 167 and 212 kDa identified with the LR8B/apoER2 antibody. The molecular mass of the band identified by the gp330 antibody was 280 kDa, a value that differs significantly from some literature values (8).

In an attempt to clarify the discrepancy in the apparent molecular weight for the prospective gp330 band, we compared our molecular weight markers (nonboiled/nonreduced Pharmacia high molecular weight standard)

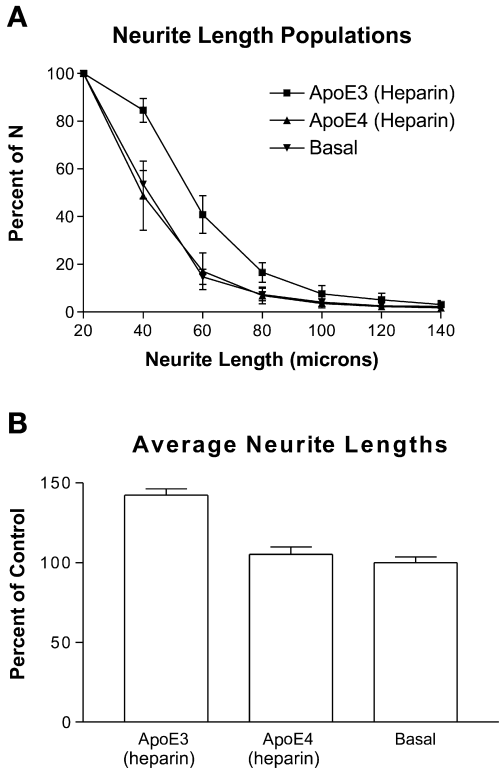

Fig. 6. Effect of antibody/heparin affinity-purified apoE phospholipid particles on neurite outgrowth in Neuro-2a cells. Neuro-2a cells were incubated with N2-supplemented control medium (dialysis/bovine serum albumin control), or in the presence of a 30 μg/ml concentration of antibody/heparin affinity-purified apoE3 or apoE4 for 48 h. Multiple phase-contrast images were captured with a ×16 objective and analyzed with the Image Tool program. Neurite extensions were determined by measuring the longest neurite from at least 300 responsive cells in duplicate experiments. A: The data were analyzed to determine the percentage of Neuro-2a cells (N) expressing neurites of defined lengths. Error bars indicate the standard deviation. B: Average neurite lengths were calculated and are shown as a percentage of control (set to 100%). The error bars indicate the standard error. The level of significance of the difference between apoE3-treated cells and control was $P = 0.0081$.

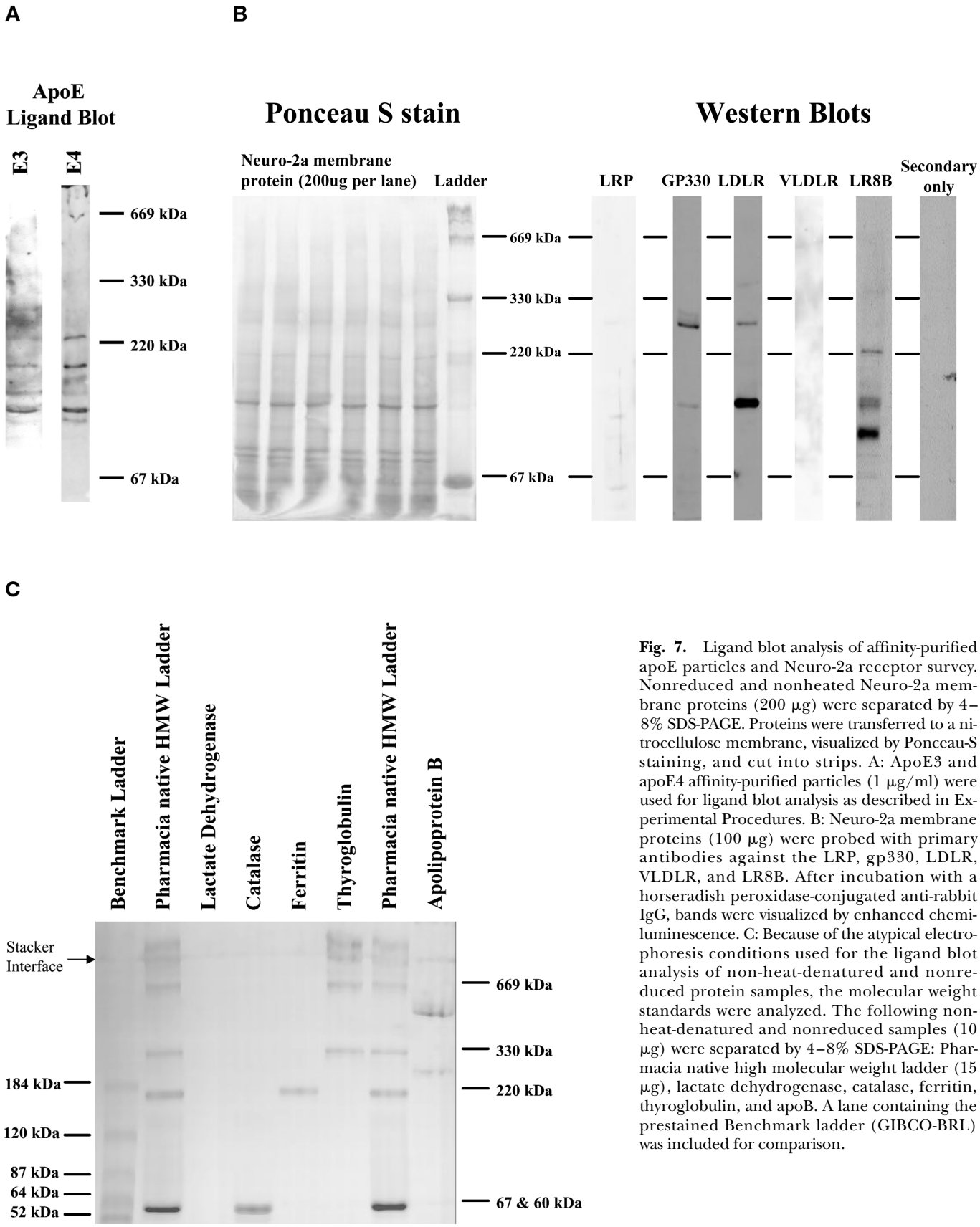

Fig. 7. Ligand blot analysis of affinity-purified apoE particles and Neuro-2a receptor survey. Nonreduced and nonheated Neuro-2a membrane proteins (200 μg) were separated by 4–8% SDS-PAGE. Proteins were transferred to a nitrocellulose membrane, visualized by Ponceau-S staining, and cut into strips. A: ApoE3 and apoE4 affinity-purified particles (1 μg/ml) were used for ligand blot analysis as described in Experimental Procedures. B: Neuro-2a membrane proteins (100 μg) were probed with primary antibodies against the LRP, gp330, LDLR, VLDLR, and LR8B. After incubation with a horseradish peroxidase-conjugated anti-rabbit IgG, bands were visualized by enhanced chemiluminescence. C: Because of the atypical electrophoresis conditions used for the ligand blot analysis of non-heat-denatured and nonreduced protein samples, the molecular weight standards were analyzed. The following non-heat-denatured and nonreduced samples (10 μg) were separated by 4–8% SDS-PAGE: Pharmacia native high molecular weight ladder (15 μg), lactate dehydrogenase, catalase, ferritin, thyroglobulin, and apoB. A lane containing the prestained Benchmark ladder (GIBCO-BRL) was included for comparison.

with molecular weight markers (GIBCO-BRL Benchmark molecular weight standards) that are traditionally used for molecular weight assessment of heat-denatured and reduced proteins (Fig. 7C). The results show a significant difference in mobility between the standards used for the traditional molecular weight assessment (boiled/reduced) as compared with the nonboiled/nonreduced standards (compare the mobility of the 184-kDa band of the Benchmark ladder with the 220-kDa band of the Pharmacia high molecular weight ladder). It may be possible that a receptor such as gp330, which contains many cysteine repeat regions, would run anomalously under these experimental conditions (nonboiled/nonreduced). Indeed, the apparent molecular weight for gp330 has been reported to vary depending on the electrophoresis conditions used. Interestingly, several of the Neuro-2a membrane proteins recognized in the apoE ligand blots have molecular masses similar to those identified in the receptor survey (gp330, 280 kDa; LDLR, 167 kDa; LR8B, 212 and 167 kDa). Each of these receptors has previously been shown to bind apoE lipoproteins (55).

DISCUSSION

The present study examined the physical and biological properties of cell-derived apoE3 and apoE4. Although compositional or size differences between the affinity-purified apoE3 or apoE4 particles were not detected, the apoE3-specific enhancement (apoE3) of neurite outgrowth was still retained in the immunoaffinity-purified particles and in particles active in binding to heparin. Analysis of the isolated particles demonstrated the absence of core lipids, and no difference in cholesterol content between apoE3 and apoE4 particles. These data indicate that the particles cannot support significant delivery of cholesterol or neutral lipid (cholesteryl ester or triglyceride), thereby diminishing the possibility that the biological activity of apoE3 particles is due to neutral lipid delivery. Furthermore, the results show that phospholipid-apoE complexes are competent to bind several membrane proteins, which on preliminary analysis may be members of the LDLR super family.

Early studies demonstrated that apoE secretion increased in response to nerve damage, a result believed to signify an important role of apoE in the redistribution of lipid during the process of neuronal remodeling (20–23). More recently, several studies have shown an isoform-specific enhancement of neurite outgrowth for cells incubated in the presence of exogenous apoE3 and rabbit β-VLDL (a large cholesteryl ester-enriched lipoprotein) (35–38). β-VLDL is an ideal lipid carrier that would be expected to efficiently supply exogenous lipid. A puzzling result from these studies was that when β-VLDL alone was added to cells, there was no stimulation of neurite outgrowth even though significant lipid delivery had occurred (41). Because of the reliance on the exogenous lipid, these studies did not identify the biologically active form of apoE, and as a consequence, the mechanism underlying the isoform-specific stimulation of neurite outgrowth could only be inferred.

Our previous studies of stably transfected Neuro-2a cells showed that an affinity-purified apoE3 particle could stimulate neurite outgrowth without the addition of an exogenous lipid source (37). One important question was whether proteins associated with apoE3 particles could be responsible for neurite outgrowth, or, conversely, a protein associated with apoE4 particles could inhibit its biological activity. Analysis of affinity-purified apoE3 and apoE4 failed to detect proteins other than apoE (Figs. 1A and 2C), suggesting that the biological activity is due to apoE3 and not associated proteins.

A key question was whether these apoE preparations contained core lipids that could support neurite outgrowth as suggested by the lipid delivery hypothesis (36, 39, 56, 57). The affinity-purified apoE preparations were shown to contain mainly phospholipid (Table 1). Characterization of the particles by NDGGE showed that most apoE particles had diameters less than 10 nm, suggesting that these particles are discoidal. Previous studies with purified apoE and apoA-I showed that the number of apolipoproteins per phospholipid particle varies in relation to the hydrated diameter (58, 59). Small-diameter particles (<12 nm) contain two molecules of protein, whereas larger (14- to 19-nm) particles had three or four. Our analysis of the purified apoE particles showed roughly 300 phospholipid molecules per apoE. This ratio is higher than some noted in the literature, but it is an average from a heterogeneous particle population with hydrated diameters varying from 7.4 to 17 nm as opposed to values obtained with purified reconstituted particles. No differences in the physical attributes of the apoE3 and apoE4 particles were detected.

ApoE3 particles were shown to stimulate neurite outgrowth whereas the apoE4 particles were neutral. Analysis of the medium at the conclusion of neurite outgrowth assays showed no changes in apoE mass or particle size distribution. Because we have shown previously that Neuro-2a cells efficiently clear apoE3 from the medium when present in large dimyristoylphosphatidylcholine disks or when present on large β-VLDL, it is likely that the small 8- to 9-nm apoE3-phospholipid complexes are taken up inefficiently by receptor-mediated endocytosis. These data, as well as the nearly identical phospholipid content of the apoE3 and apoE4 particles, argue that the apoE3-specific stimulation of neurite outgrowth is not due to apoE3-mediated delivery of phospholipids.

The importance of heparan sulfate proteoglycan in apoE-related biological systems has been well documented (49, 51, 52). It has been shown that affinity of apoE for heparin is an important determinant for high affinity localization to the cell surface (52). We showed that the affinity-purified apoE3 and apoE4 phospholipid particles readily bound to heparin (Fig. 5). In addition, particles competent to bind heparin were shown to maintain the same isoform-specific effects on neurite outgrowth (Fig. 6). Thus, the isoform-specific effect is not reflected in a differential interaction of apoE3 and apoE4 particles with heparin. Whether the ability to bind to heparin or cell surface proteoglycan is necessary for apoE3 stimulated neurite outgrowth remains to be tested.

Because several RAP inhibition studies implicated member(s) of the LDLR family in mediating the apoE3 biological activity, we investigated whether affinity-purified apoE particles could bind to Neuro-2a membrane proteins. Ligand blot analysis showed that the apoE particles bound to several membrane proteins that aligned perfectly with bands detected via Western blots using antibodies to LDLR family members, including LR8B/apoER2 (167 and 212 kDa), LDLR (167 kDa), and gp330 (280 kDa). This is an intriguing result because these receptors have been implicated as components of signal transduction cascades (60–62). MDab1, a signal transduction adaptor protein, has been shown to bind to the cytoplasmic tails of the LDLR, LRP, LR8B/apoER2, VLDLR, and gp330 (61, 62). Importantly, the report by Trommsdorff et al. (62) suggests that LR8B/apoER2 and the VLDLR participate in neuronal migration and patterning during development as components of a signal transduction pathway. Thus, it is interesting to speculate that the apoE3-phospholipid complexes stimulate neurite outgrowth by initiating a signaling pathway through one or more of the apoE receptors expressed by Neuro-2a cells. In this regard, previous studies have shown apoE to have hormone- or cytokine-like effects in steroidogenic cells (63, 64), platelets (65), and lymphocytes (66). Thus, there is significant precedent to speculate that cytokine-like effects of apoE in Neuro-2A cells may underlie the stimulation of neurite outgrowth. Although we did not identify any prominent differences in the binding of apoE3 and apoE4 particles on the ligand blots, further studies to test for such differences in cell based assays are clearly warranted.

We did not detect expression of either the LRP or the VLDLR in the Neuro-2a membrane protein extracts. Several studies have implicated the LRP as a key component in the apoE induction of neurite outgrowths (36, 40, 41). Although the possibility remains that Neuro-2a cells express LRP at levels below our detection limit, the apoE ligand blots also did not identify a protein within the LRP size range. The potential participation of the LRP in the neurite outgrowth process is inferred from results showing that antibodies to the LRP inhibit the process (36, 40). However, potential cross-reactivity between the LRP antibodies and other LDLR family members expressed by Neuro-2a cells has not been evaluated. Studies have shown that LRP, gp330, and LR8B/apoER2 can bind similar cytosolic binding proteins, a result that may reflect potential redundancy for signaling (67).

Although our in vitro results imply that lipid delivery is not important for neurite outgrowth, an in vivo study demonstrates that it is needed for the removal of excess lipid after neuronal injury (68). An interesting model presents itself if we combine both the in vitro and in vivo observations. It is possible that after CNS injury, astrocyte-derived apoE performs dual roles. The phospholipid-apoE complex could act as both a signaling molecule, to facilitate neurite outgrowth and neuronal repair, and, after fusion or transfer to larger particles, as a lipid scavenger to clear cellular debris.

This work was supported by NIH grants HL 32868 and HL 49373. R.B.D. was partially supported by a predoctoral fellowship from the Institute for Cell and Developmental Biology, State University of New York at Stony Brook. We thank D. K. Strickland and J. Nimpf for kindly supplying antibodies, and Fayanne Thorngate for helpful comments and suggestions.

Manuscript received 11 December 2000 and in revised form 20 February 2001.

REFERENCES

1. Shore, B., and V. Shore. 1973. Heterogeneity of human plasma very low density lipoproteins. Separation of species differing in protein components. *Biochemistry.* **12:** 502–507.
2. Brown, M. S., and J. L. Goldstein. 1986. A receptor-mediated pathway for cholesterol homeostasis. *Science.* **232:** 34–47.
3. Weisgraber, K. H. 1994. Apolipoprotein E: structure-function relationships. *Adv. Protein Chem.* **45:** 249–302.
4. Blue, M-L., D. L. Williams, S. Zucker, S. A. Khan, and C. B. Blum. 1983. Apolipoprotein E synthesis in human kidney, adrenal gland, and liver. *Proc. Natl. Acad. Sci.USA.* **80:** 283–287.
5. Elshourbagy, N. A., W. S. Liao, R. W. Mahley, and J. M. Taylor. 1985. Apolipoprotein E mRNA is abundant in the brain and adrenal, as well as in the liver and is present in other peripheral tissues of rats and marmosets. *Proc. Natl. Acad. Sci. USA.* **82:** 203–207.
6. Williams, D. L., P. A. Dawson, T. C. Newman, and L. L. Rudel. 1985. Apolipoprotein E synthesis in peripheral tissues of nonhuman primates. *J. Biol. Chem.* **260:** 2444–2451.
7. Newman, T. C., P. A. Dawson, L. L. Rudel, and D. L. Williams. 1985. Quantitation of apolipoprotein E messenger RNA in the liver and peripheral tissues of nonhuman primates. *J. Biol. Chem.* **260:** 2452–2457.
8. Hussain, M. M., D. K. Strickland, and A. Bakillah. 1999. The mammalian low-density lipoprotein receptor family. *Annu. Rev. Nutr.* **19:** 141–172.
9. Krul, E. S., and J. Tang. 1992. Secretion of apolipoprotein E by an astrocytoma cell line. *J. Neurosci. Res.* **32:** 227–238.
10. Herscovitz, H., D. Gantz, A. M. Tercyak, V. I. Zannis, and D. M. Small. 1992. Expression of human apolipoprotein E but not that of apolipoprotein A-I by mouse C127 cells is associated with increased secretion of lipids in the form of vesicles and discs. *J. Lipid Res.* **33:** 791–803.
11. Zhang, W-Y., P. M. Gaynor, and H. S. Kruth. 1996. Apolipoprotein E produced by human monocyte-derived macrophages mediates cholesterol efflux that occurs in the absence of added cholesterol acceptors. *J. Biol. Chem.* **271:** 28641–28646.
12. Smith, J. D., M. Miyata, M. Ginsberg, C. Grigaux, E. Shmookler, and A. S. Plump. 1996. Cyclic AMP induces apolipoprotein E binding activity and promotes cholesterol efflux from a macrophage cell line to apolipoprotein acceptors. *J. Biol. Chem.* **271:** 30647–30655.
13. Zannis, V. I., J. L. Breslow, G. Utermann, R. W. Mahley, K. H. Weisgraber, R. J. Havel, J. L. Goldstein, M. S. Brown, G. Schonfeld, W. R. Hazzard, and C. Blum. 1982. Proposed nomenclature of apoE isoproteins, apoE genotypes, and phenotypes. *J. Lipid Res.* **23:** 911–914.
14. Boyles, J. K., R. E. Pitas, E. Wilson, R. W. Mahley, and J. M. Taylor. 1985. Apolipoprotein E associated with astrocytic glia of the central nervous system and with nonmyelinating glia of the peripheral nervous system. *J. Clin. Invest.* **76:** 1501–1513.
15. Pitas, R. E., J. K. Boyles, S. H. Lee, D. Foss, and R. W. Mahley. 1987. Astrocytes synthesize apolipoprotein E and metabolize apolipoprotein E-containing lipoproteins. *Biochim. Biophys. Acta.* **917:** 148–161.
16. Stone, D. J., I. Rozovsky, T. E. Morgan, C. P. Anderson, H. Hajian, and C. E. Finch. 1997. Astrocytes and microglia respond to estrogen with increased apoE mRNA in vivo and in vitro. *Exp. Neurol.* **143:** 313–318.
17. Nakai, M., T. Kawamata, K. Maeda, and C. Tanaka. 1996. Expression of apoE mRNA in rat microglia. *Neurosci. Lett.* **211:** 41–44.
18. Roheim, P. S., M. Carey, T. Forte, and G. L. Vega. 1979. Apolipoproteins in human cerebrospinal fluid. *Proc. Natl. Acad. Sci. USA.* **76:** 4646–4649.
19. Carlsson, J., V. W. Armstrong, H. Reiber, K. Felgenhauer, and D. Seidel. 1991. Clinical relevance of the quantification of apolipoprotein E in cerebrospinal fluid. *Clin. Chim. Acta.* **196:** 167–176.

20. Dawson, P. A., N. Schechter, and D. L. Williams. 1986. Induction of rat E and chicken A-1 apolipoproteins and mRNAs during optic nerve degeneration. *J. Biol. Chem.* **261:** 5681–5684.
21. Ignatius, M. J., P. J. Gebickle-Harter, J. H. P. Skene, J. W. Schilling, K. H. Weisgraber, R. W. Mahley, and E. M. Shooter. 1986. Expression of apolipoprotein E during nerve degeneration and regeneration. *Proc. Natl. Acad. Sci. USA.* **83:** 1125–1129.
22. Ignatius, M. J., E. M. Shooter, R. E. Pitas, and R. W. Mahley. 1987. Lipoprotein uptake by neuronal growth cones in vitro. *Science.* **236:** 959–962.
23. Boyles, J. K., L. M. Notterpek, and L. J. Anderson. 1990. Accumulation of apolipoproteins in the regenerating and remyelinating mammalian peripheral nerve. Identification of apolipoprotein D, apolipoprotein A-IV, apolipoprotein E, and apolipoprotein A-I. *J. Biol. Chem.* **265:** 17805–17815.
24. Rebeck, G. W., J. S. Reiter, D. K. Strickland, and B. T. Hyman. 1993. Apolipoprotein E in sporadic Alzheimer's disease: allelic variation and receptor interactions. *Neuron.* **11:** 575–580.
25. Strittmatter, W. J., K. H. Weisgraber, D. Y. Huang, L-M. Dong, G. S. Salvesen, M. Pericak-Vance, D. Schmechel, A. M. Saunders, D. Goldgaber, and A. D. Roses. 1993. Binding of human apolipoprotein E to synthetic amyloid β peptide: isoform-specific effects and implications for late-onset Alzheimers disease. *Proc. Natl. Acad. Sci. USA.* **90:** 8098–8102.
26. Goedert, M., W. Strittmatter, and A. Roses. 1994. Risky apolipoprotein in brain. *Nature.* **372:** 45–46.
27. Strittmatter, W., K. Weisgraber, M. Goedert, A. Saunders, D. Huang, E. Corder, L-M. Dong, R. Jakes, M. Alberts, J. Gilbert, S-H. Han, C. Hulette, G. Einstein, D. Schmechel, M. Pericak-Vance, and A. Roses. 1994. Hypothesis: microtubule instability and paired helical filament formation in the Alzheimer disease brain are related to apolipoprotein E genotype. *Exp. Neurol.* **125:** 163–171.
28. Wisniewski, T., and B. Frangione. 1992. Apolipoprotein E: a pathological chaperone protein in patients with cerebral and systemic amyloid. *Neurosci. Lett.* **135:** 235–238.
29. Strittmatter, W. J., A. M. Saunders, D. Schmechel, M. Pericak-Vance, I. Enchild, G. S. Salvesen, and A. D. Roses. 1993. Apolipoprotein E: high-avidity binding to β-amyloid and increased frequency of type 4 allele in late onset Alzheimer's disease. *Proc. Natl. Acad. Sci. USA.* **90:** 1977–1981.
30. LaDu, M. J., M. T. Falduto, A. M. Manelli, C. A. Reardon, G. S. Getz, and D. E. Frail. 1994. Isoform-specific binding of apolipoprotein E to β-amyloid. *J. Biol. Chem.* **269:** 23403–23406.
31. Bales, K. R., V. Verina, R. C. Dodel Y. Du, L. Altstiel, M. Bender, P. Hyslop, E. M. Johnstone, S. P. Little, D. J. Cumins, P. Piccardo, B. Ghetti, and H. E. Paulus. 1997. Lack of apolipoprotein E dramatically reduces amyloid beta-peptide deposition. *Nat. Genet.* **17:** 263–264.
32. Holtzman, D. M., K. R. Bales, S. Wu, P. Bhat, M. Parsadanian, A. M. Fagan, L. K. Chang, Y. Sun, and S. M. Paul. 1999. In-vivo expression of apolipoprotein E reduces amyloid-beta deposition in a mouse model of Alzheimer's disease. *J. Clin. Invest.* **103:** R15–R21.
33. DeMattos, R. B., F. E. Thorngate, and D. L. Williams. 1999. A test of the cytosolic apolipoprotein E hypothesis fails to detect the escape of apolipoprotein E from the endocytic pathway into the cytosol and shows that direct expression of apolipoprotein E in the cytosol is cytotoxic. *J. Neurosci.* **19:** 2464–2473.
34. Strittmatter, W. J., A. M. Saunder, M. Goedert, K. H. Weisgraber, L. M. Dong, R. Jakes, D. Y. Huang, M. Pericak-Vance, D. Schmechel, and A. D. Roses. 1994. Isoform-specific interactions of apolipoprotein E with microtubule-associated protein tau: implications for Alzheimer's disease. *Proc. Natl. Acad. Sci. USA.* **91:** 11183–11186.
35. Nathan, B. P., K-C. Chang, S. Bellosta, E. Brisch, N. Ge, R. W. Mahley, and R. E. Pitas. 1995. The inhibitory effect of apolipoprotein E4 on neurite outgrowth is associated with microtubule depolymerization. *J. Biol. Chem.* **270:** 19797–19799.
36. Holtzman, D. M., R. E. Pitas, J. Kilbridge, B. Nathan, R. W. Mahley, G. Bu, and A. L. Schwartz. 1995. Low density lipoprotein receptor-related protein mediates apolipoprotein E-dependent neurite outgrowth in a central nervous system-derived neuronal cell line. *Proc. Natl. Acad. Sci. USA.* **92:** 9480–9484.
37. DeMattos, R. B., L. K. Curtiss, and D. L. Williams. 1998. A minimally-lipidated form of cell-derived apolipoprotein E exhibits isoform-specific stimulation of neurite outgrowth in the absence of exogenous lipids or lipoproteins. *J. Biol. Chem.* **273:** 4206–4212.
38. Sun, Y., S. Wu, G. Bu, M. K. Onifade, S. N. Patel, M. J. LaDu, A. M. Fagan, and D. M. Holtzman. 1998. Glial fibrillary acidic protein-apolipoprotein E (apoE) transgenic mice: astrocyte-specific expression and differing biological effects of astrocyte-secreted apoE3 and apoE4 lipoproteins. *J. Neurosci.* **18:** 3261–3272.
39. Handelmann, G. E., J. K. Boyles, K. H. Weisgraber, R. W. Mahley, and R. E. Pitas. 1992. Effects of apolipoprotein E, β-very low density lipoproteins, and cholesterol on the extension of neurites by rabbit dorsal root ganglion neurons in vitro. *J. Lipid Res.* **33:** 1677–1688.
40. Fagan, A. M., G. Bu, Y. Sun, A. Daugherty, and D. M. Holtzman. 1996. Apolipoprotein E-containing high density lipoprotein promotes neurite outgrowth and is a ligand for the low density lipoprotein receptor-related protein. *J. Biol. Chem.* **271:** 30121–30125.
41. Bellosta, S., B. P. Nathan, M. Orth, L-M. Dong, R. W. Mahley, and R. E. Pitas. 1995. Stable expression and secretion of apolipoprotein E3 and E4 in mouse neuroblastoma cells produces differential effects on neurite outgrowth. *J. Biol. Chem.* **270:** 27063–27071.
42. McCall, M. R., T. M. Forte, and V. G. Shore. 1988. Heterogeneity of nascent high density lipoproteins secreted by the hepatoma-derived cell line, Hep G2. *J. Lipid Res.* **29:** 1127–1137.
43. Kurantz, M. J., R. J. Maxwell, R. Kwoczak, and F. Taylor. 1991. Rapid and sensitive method for the quantitation of nonpolar lipids by high-performance thin-layer chromatography and fluorodensitometry. *J. Chromatogr.* **549:** 387–399.
44. Metcalfe, L. D., A. A. Schmitz, and J. R. Pelka. 1966. Rapid preparation of fatty acid esters from lipids for gas chromatographic analysis. *Anal. Chem.* **38:** 514–515.
45. Wolfe, M. S., J. S. Parks, T. M. Morgan, and L. L. Rudel. 1993. Childhood consumption of polyunsaturated fat lowers risk for coronary artery atherosclerosis in African green monkey. *Arterioscler. Thromb. Vasc. Biol.* **13:** 863–875.
46. Lowry, O. H., N. J. Rosebrough, A. L. Farr, and R. J. Randall. 1951. Protein measurement with the Folin phenol reagent. *J. Biol. Chem.* **193:** 265–275.
47. Innerarity, T. L., R. E. Pitas, and R. W. Mahley. 1979. Binding of arginine-rich (E) apoprotein after recombination with phospholipid vesicles to the low density lipoprotein receptors of fibroblasts. *J. Biol. Chem.* **254:** 4186–4190.
48. Ridgway, N. D., D. M. Byers, H. W. Cook, and M. K. Storey. 1999. Integration of phospholipid and sterol metabolism in mammalian cells. *Prog. Lipid Res.* **38:** 337–360.
49. Ji, Z-S., S. Fazio, Y-L. Lee, and R. W. Mahley. 1994. Secretion-capture role for apolipoprotein E in remnant lipoprotein metabolism involving cell surface heparan sulfate proteoglycans. *J. Biol. Chem.* **269:** 2764–2772.
50. Williams, K. J., and I. V. Fuki. 1997. Cell-surface heparan sulfate proteoglycans: dynamic molecules mediating ligand catabolism. *Curr. Opin. Lipidol.* **8:** 253–262.
51. Ji, Z. S., H. L. Dichek, R. D. Miranda, and R. W. Mahley. 1997. Heparan sulfate proteoglycans participate in hepatic lipase and apolipoprotein E-mediated binding and uptake of plasma lipoproteins, including high density lipoproteins. *J. Biol. Chem.* **272:** 31285–31292.
52. Burgess, J. W., D. R. Gould, and Y. L. Marcel. 1998. The HepG2 extracellular matrix contains separate heparinase- and lipid-releasable pools of apoE. Implications for hepatic lipoprotein metabolism. *J. Biol. Chem.* **273:** 5645–5654.
53. Schneider, W. J., U. Beisiegel, J. L. Goldstein, and M. S. Brown. 1982. Purification of the low density lipoprotein receptor, an acidic glycoprotein of 164,000 molecular weight. *J. Biol. Chem.* **257:** 2664–2673.
54. Novak, S., T. Hiesberger, W. J. Schneider, and J. Nimpf. 1996. A new low density lipoprotein receptor homologue with 8 ligand binding repeats in brain of chicken and mouse. *J. Biol. Chem.* **271:** 11732–11736.
55. St.Clair, R. W., and U. Beisiegel. 1997. What do all the apolipoprotein E receptors do? *Curr. Opin. Lipidol.* **8:** 243–245.
56. Nathan, B. P., S. Bellosta, D. A. Sanan, K. H. Weisgraber, R. W. Mahley, and R. E. Pitas. 1994. Differential effects of apolipoproteins E3 and E4 on neuronal growth in vitro. *Science.* **264:** 850–852.
57. Poirier, J., A. Minnich, and J. Davignon. 1995. Apolipoprotein E, synaptic plasticity and Alzheimer's disease. *Ann. Med.* **27:** 663–670.
58. Wald, J. H., E. S. Krul, and A. Jonas. 1990. Structure of apolipoprotein A-I in three homogenous, reconstituted high density lipoprotein particles. *J. Biol. Chem.* **265:** 20037–20043.
59. De Pauw, M., B. Vanloo, K. H. Weisgraber, and M. Rosseneu. 1995. Comparison of lipid-binding and lecithin:cholesterol acyltransferase activation of the amino- and carboxyl-terminal domains of human apolipoprotein E3. *Biochemistry.* **34:** 10953–10960.

60. Hjalm, G., E. Murray, G. Crumley, W. Harazim, S. Lundgren, I. Onyango, B. Ek, M. Larsson, C. Juhlin, P. Hellman, H. Davis, G. Akerstrom, L. Rask, and B. Morse. 1996. Cloning and sequencing of human gp330, a Ca(2+)-binding receptor with potential intracellular signaling properties. *J. Biol. Chem.* **239:** 132–137.
61. Trommsdorff, M., J. P. Borg, B. Margolis, and J. Herz. 1998. Interaction of cytosolic adaptor proteins with neuronal apolipoprotein E receptors and the amyloid precursor protein. *J. Biol. Chem.* **273:** 33556–33560.
62. Trommsdorff, M., M. Gotthardt, T. Hiesberger, J. Shelton, W. Stockinger, J. Nimpf, R. E. Hammer, and J. A. Richardson. 1999. Reeler/disabled-like disruption of neuronal migration in knockout mice lacking the VLDL receptor and apoE receptor 2. *Cell.* **97:** 689–701.
63. Reyland, M. E., and D. L. Williams. 1991. Suppression of cAMP-mediated signal transduction in mouse adrenocortical cells which express apolipoprotein E. *J. Biol. Chem.* **266:** 21099–21194.
64. Dyer, C. A., and L. K. Curtiss. 1988. Apoprotein E-rich high density lipoprotein inhibit ovarian androgen synthesis. *J. Biol. Chem.* **263:** 10965–10973.
65. Riddell, D. R., A. Graham, and J. S. Owen. 1997. Apolipoprotein E inhibits platelet aggregation through the L-arginine: nitric oxide pathway. Implications for vascular disease. *J. Biol. Chem.* **272:** 89–95.
66. Pepe, M. G., and L. K. Curtiss. 1986. Apolipoprotein E is a biologically active contituent of the normal immunoregularity lipoprotein, LDL-In. *J. Immunol.* **136:** 3716–3723.
67. Gotthardt, M., M. Trommsdorff, M. F. Nevitt, J. Shelton, J. A. Richardson, W. Stockinger, J. Nimpf, and J. Herz. 2000. Interactions of the low density lipoprotein gene family with cytosolic adaptor and scaffold proteins suggest diverse biological functions in cellular communication and signal transduction. *J. Biol. Chem.* **275:** 25616–25624.
68. Fagan, A. M., B. A. Murphy, S. N. Patel, J. F. Kilbridge, W. C. Mobley, G. Bu, and D. M. Holtzman. 1998. Evidence for normal aging of the septo-hippocampal cholinergic system in apoE (−/−) mice but imparied clearence of axonal degeneration products following injury. *Exp. Neurol.* **151:** 314–325.